# Theory of one-phonon resonant Raman scattering in a magnetic field

C. Trallero-Giner,* T. Ruf, and M. Cardona
*Max-Planck-Institut für Festkörperforschung, Heisenbergstrasse 1, Postfach 80 06 65, D-7000 Stuttgart 80, Federal Republic of Germany*
(Received 26 June 1989; revised manuscript received 12 October 1989)

A theory of one-phonon resonant Raman scattering in diamond- and zinc-blende-type semiconductors in a magnetic field is developed. We consider the deformation-potential and Fröhlich interactions for the electron–one-phonon coupling. Explicit expressions for the Raman efficiency as a function of the laser energy $\hbar\omega_l$ and the applied magnetic field $H$ are given. The Landau levels and the spin splitting are considered in the framework of the envelope-function approximation using a three-band parabolic model. In both types of electron-phonon interaction, the Raman intensity as a function of $\hbar\omega_l$ and $H$ shows a set of incoming and outgoing resonances corresponding to different interband magneto-optical transitions. Selection rules and conditions for double resonance are deduced for different scattering configurations with circularly polarized light. An extension of the theory to consider an admixed-valence-level structure is outlined. On these grounds the essential features of recent magneto-Raman experiments discussed in the following paper can be explained.

## I. INTRODUCTION

Recently, it has been demonstrated, that one-phonon resonant Raman scattering (RRS) in a magnetic field is a useful technique to obtain enhanced sensitivity for the observation of interband transitions in semiconductors.[1–3] The sharpening of resonant features due to the one-dimensional density of states as introduced by the external magnetic field $H$ together with the modulation spectroscopy aspects of resonant Raman scattering[4] lead to strong oscillations in the scattering efficiencies. The intensity of the Stokes Raman LO phonon as a function of $H$ can be interpreted in terms of band-structure properties and electron-phonon interaction: The quantitative assignment of interband transitions to experimental resonances provides a test for sophisticated band theories[5–8] and enhances our understanding of the complicated valence-level structure. The observation of resonant magnetopolaron effects in InP (Ref. 3) highlights the impact of electron-phonon interaction in polar semiconductors. Resonances in different scattering configurations can be attributed to Raman processes mediated by deformation potential or Fröhlich interaction.

This qualitative picture for the Raman processes, however, is not sufficient to understand problems such as those of incoming and outgoing resonances and their relative strengths or possible conditions for magnetic-field-induced double resonances. In order to obtain a consistent description of the resonances observed in different scattering configurations with circularly polarized light one has to go beyond the assignment of experimental features to theoretical interband magneto-optical transitions: a theoretical model for one-phonon RRS in a magnetic field, which includes different mechanisms for electron-phonon interaction, is necessary. In the past interband and intraband light scattering in a magnetic field has been investigated theoretically in the context of electronic scattering processes or cyclotron-phonon resonances.[9–15] In Ref. 16 the cross section for first-order Raman scattering in a magnetic field considering the deformation potential as the electron-phonon coupling mechanism was calculated within a two-band model. The results obtained there cannot be used to explain the above-mentioned features of the one-phonon RRS spectra. Double resonances, for example, cannot be obtained in a two-band model, since the two denominators which appear in the scattering efficiency (incoming and outgoing resonances) never vanish simultaneously for the same Landau $n$.

In this paper we develop a theory of one-phonon RRS in diamond- and zinc-blende-type semiconductors in a magnetic field in which deformation-potential and Fröhlich interactions are considered to mediate the electron-phonon interaction. It is organized in the following way: In Sec. II we introduce some general relations concerning the Raman efficiency and the band model we use; the case of deformation-potential interaction is considered in Sec. III where selection rules for one-phonon RRS in different scattering configurations are studied and the double-resonance condition is analyzed; Sec. IV is devoted to Fröhlich interaction. An extension of the theory is made in Sec. V in order to take the mixing of valence levels and a realistic band structure into account. Theoretical results obtained from this are briefly compared to experimental spectra. Section VI presents the conclusions.

## II. THEORY OF ONE-PHONON RRS IN A MAGNETIC FIELD

To calculate the one-phonon RRS cross section we consider a model with parabolic nondegenerate bands and uncorrelated electron-hole pairs as excited states. Figure 1(a) schematically shows the band structure and

 

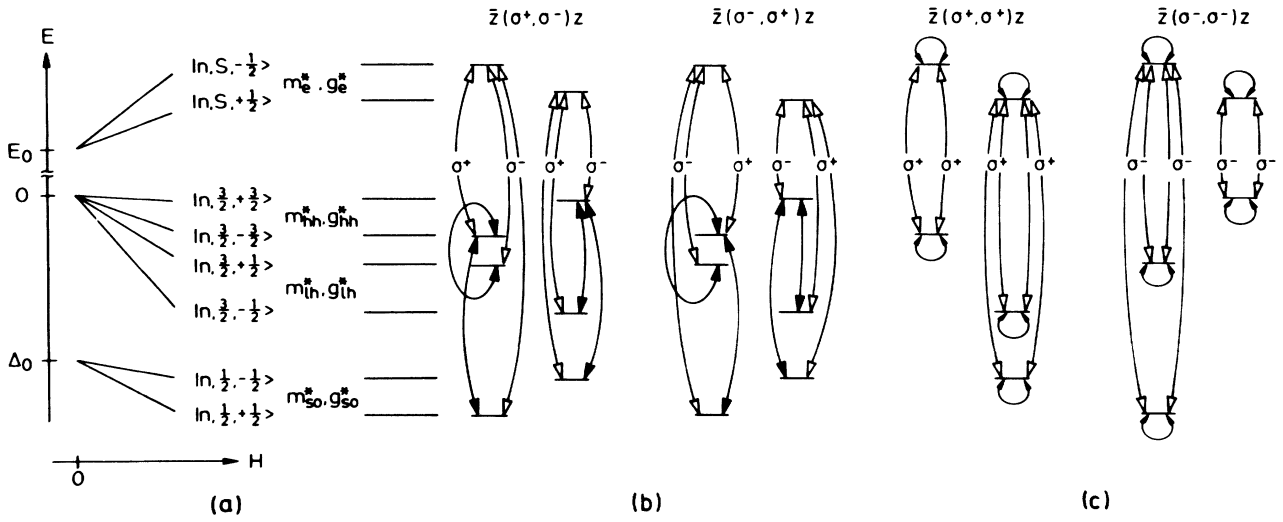


FIG. 1. Terms contributing to the Raman efficiency in a magnetic field for a zinc-blence-type semiconductor in the vicinity of $E_0$ and $E_0+\Delta_0$ critical points in the simple parabolic band model. (a) Parameters used to describe band structure and Landau levels as a function of magnetic field. (b) Transitions between Landau levels which contribute to Raman processes in the $\bar{z}(+,-)z$ and $\bar{z}(-,+)z$ scattering configurations: deformation-potential interaction. (c) Idem for the $\bar{z}(+,+)z$ and $\bar{z}(-,-)z$ scattering configurations: Fröhlich interaction. Open arrows represent interband magneto-optical transitions, solid arrows the transitions mediated by the electron-phonon interaction.

the parameters used for its description which can be applied to a zinc-blende-type semiconductor in the vicinity of the $E_0$ and $E_0+\Delta_0$ critical points.

### A. Hamiltonian of the system

The total Hamiltonian is given by

$$\mathcal{H}=H_0+H_{E\text{-}R}+H_{E\text{-}P} \ . \tag{1}$$

$H_{E\text{-}R}$ and $H_{E\text{-}P}$ are the electron-radiation and electron-phonon interaction Hamiltonians, respectively. $H_0$ is the unperturbed Hamiltonian equal to

$$H_0=\sum_{\kappa,\mathbf{e}}\hbar\omega(a^{\dagger}_{\kappa,\mathbf{e}}a_{\kappa,\mathbf{e}}+\tfrac{1}{2})+\sum_{\mathbf{q}}\hbar\omega_0(\mathbf{q})(b^{\dagger}_{\mathbf{q}}b_{\mathbf{q}}+\tfrac{1}{2}) +\sum_{\alpha,i}E_{\alpha,i}(d^{\dagger}_{\alpha,i}d_{\alpha,i}+\tfrac{1}{2}) \tag{2}$$

corresponding to the free photon, phonon, and electron fields, respectively. In Eq. (2), $a^{\dagger}_{\kappa,\mathbf{e}}$ and $b^{\dagger}_{\mathbf{q}}$ represent the creation operators for photons and phonons, $\kappa$ and $\mathbf{e}$ are the wave vector and polarization of the light with frequency $\omega$, and $\omega_0$ is the frequency of a phonon with wave vector $\mathbf{q}$. $d^{\dagger}_{\alpha,i}$ is the creation operator for an electron in the band $i$ with quantum number $\alpha$ and energy $E_{\alpha,i}$. For an electron in the band $i$ with a constant magnetic field $H$ parallel to the $\hat{\mathbf{z}}$ axis and in the framework of the envelope-function approximation, the $E_{\alpha,i}$ are the eigenvalues of the equation

$$\left[-\frac{\hbar^2\nabla^2}{2m_i^*}-i\frac{\hbar eH}{m_i^*c}y\frac{\partial}{\partial x}+\frac{m_i^*\omega_{ci}^2}{2}y^2+\frac{\mu_B\sigma_z}{2}g_i^*\right]\Psi_\alpha =E_{\alpha,i}\Psi_\alpha \ , \tag{3}$$

where $\sigma_z$ is a Pauli matrix and $\mu_B$ is the Bohr magneton. $\omega_{ci}$, $m_i^*$, and $g_i^*$ are the cyclotron frequency, the effective mass, and the $g$ factor of the electron in the band $i$, respectively. In this case the quantum number $\alpha$ includes $n$, $k_x$, $k_z$, and $m_s=\pm\frac{1}{2}$ for the two different spin states. From Eq. (3) it follows that the energies $E_{n_i,k_{iz}}$ and the electron wave functions $\Psi$ are given by

$$E_{n_i,k_{iz},m_{si}}=\frac{\hbar^2k_{iz}^2}{2m_i^*}+\hbar\omega_{ci}(n_i+\tfrac{1}{2})+\mu_BHg_i^*m_{si} \ ,$$

$$\text{with } n_i=0,1,\ldots, \tag{4}$$

$$\Psi_{n_i,\mathbf{k}_i,m_{si}}(\mathbf{r})=V^{-1/3}e^{i\mathbf{k}_i\cdot\rho}\Phi_{n_i}(y)u_{i,0}(\mathbf{r}) \ , \tag{5}$$

where $u_{i,0}$ is the electron Bloch function in the band $i$ for $\mathbf{k}=0$, $\Phi_{n_i}$ are the harmonic oscillator functions, $V$ is the volume of the crystal, and $\rho=(x,z)$.

The electron-radiation interaction Hamiltonian can be expressed in the dipole approximation by

$$H_{E\text{-}R}=\sum_{\kappa,\mathbf{e}}(a_{\kappa,\mathbf{e}}+a^{\dagger}_{-\kappa,\mathbf{e}}\frac{|e|}{m_0}\left[\frac{2\pi\hbar}{V\omega n^2}\right]^{1/2}\mathbf{e}\cdot\mathbf{p} \ , \tag{6}$$

$m_0$ and $e$ being the free-electron mass and charge, $n$ the refractive index, $\mathbf{p}$ the momentum operator, and $\mathbf{e}$ the polarization of the photon field. If we consider the direct-allowed electron transition between two bands $i,j$ and make use of the wave function (5), the matrix element $\langle j|H_{E\text{-}R}|i\rangle$ can be written as

$$\langle j|H_{E\text{-}R}|i\rangle=\frac{|e|}{m_0}\left[\frac{2\pi\hbar}{V\omega n^2}\right]^{1/2}\mathbf{e}\langle j|\mathbf{p}|i\rangle \times\delta_{\mathbf{k}_j,\mathbf{k}_i\pm\kappa}\delta_{n_i,n_j} \tag{7}$$

In Eq. (7) the $\pm$ signs correspond to the absorption or emission of one photon by the electron.

Since first-order Raman scattering involves one step mediated by electron-phonon interaction, the corresponding Hamiltonian is linear in the phonon operator and bilinear in the electron operator, that is,

$$H_{E\text{-}P}=\sum_{\substack{\alpha,\alpha'\\ i,j\\ \mathbf{q}}}[S_{\alpha,i}^{\alpha',j}(\mathbf{q})d_{\alpha',j}^{\dagger}d_{\alpha,i}b_{\mathbf{q}}^{\dagger}]+\text{c.c.}\ , \tag{8}$$

where $S_{\alpha,i}^{\alpha',j}$ is the electron-hole pair to phonon coupling constant. In this paper two different mechanisms of electron-phonon coupling which contribute to the Raman cross section will be investigated: the dipole-allowed deformation-potential (short-range) and the intrinsic dipole-forbidden Fröhlich (long-range) electron-phonon interaction.[17]

### B. Raman scattering efficiency

The Raman scattering efficiency $dS/d\Omega$ per unit length and unit solid angle $d\Omega$ and the scattering amplitude per unit time $W_{\mathrm{FI}}$ are related by the equation

$$\frac{dS}{d\Omega}=\frac{\omega_l\omega_s^3}{(2\pi)^2}\frac{n_l n_s^3}{c^4}\frac{V}{(\hbar\omega_l)^2}|W_{\mathrm{FI}}(\omega_s,\mathbf{e}_s;\omega_l,\mathbf{e}_l)|^2\ . \tag{9}$$

In the initial state $|I\rangle$ of the system there is an incident photon of frequency $\omega_l$ and polarization $\mathbf{e}_l$; the final state $|F\rangle$ has a photon of frequency $\omega_s=\omega_l-\omega_0$ and a phonon $\omega_0$. In the following the indices $l$ and $s$ always refer to incoming (laser) and scattered (Stokes) light, respectively. Using Eqs. (1)–(4) in lowest-order perturbation theory the scattering amplitude for a semiconductor in a magnetic field can be written as

$$W_{\mathrm{FI}}=\sum_{\mu_i,\mu_j}\frac{\langle F|H_{E\text{-}R}|\mu_j\rangle\langle\mu_j|H_{E\text{-}P}|\mu_i\rangle\langle\mu_i|H_{E\text{-}R}|I\rangle}{(\hbar\omega_s-E_{\mu_j}+i\Gamma_{\mu_j})(\hbar\omega_l-E_{\mu_i}+i\Gamma_i)}$$
$$+\text{five nonresonant terms}\ . \tag{10}$$

The indices $\mu_k$ $(k=i,j)$ refer to intermediate electron-hole pair states with lifetime broadenings $\Gamma_k$ and energies

$$E_{\mu_k}=E_{g_k}+\frac{\hbar^2k_{ez}^2}{2m_e^*}+\frac{\hbar^2k_{hz}^2}{2m_{h_k}^*}+\hbar\omega_{ce}(n_e+\tfrac{1}{2})$$
$$+\hbar\omega_{ch_k}(n_{h_k}+\tfrac{1}{2})+\mu_B H(g_e^* m_{se}-g_{h_k}^* m_{sh_k}) \tag{11}$$

with $E_{g_k}$ being the energy of the gap associated with the valence band $k$ and the conduction band and $m_e^*$ ($m_{h_k}^*$) the effective electron (hole) mass. In Eq. (10) the first term dominates for laser energies near interband critical points. The other ones are nonresonant and only cause a small background. Therefore they shall be neglected in the following.

## III. DIPOLE-ALLOWED DEFORMATION-POTENTIAL INTERACTION

To calculate the Raman efficiency in a magnetic field we choose a three-band model consisting of the conduction band ($c$) and two valence bands ($v_i$ and $v_j$). In this case the electron-hole pair phonon coupling constant is equal to[18]

$$S_{\alpha,i}^{\alpha',j}(\mathbf{q})=\frac{u_0\sqrt{3}}{2a_0}\langle\alpha',j|D_e(\mathbf{r}_e)e^{i\mathbf{q}\cdot\mathbf{r}_e}-D_h(\mathbf{r}_h)e^{i\mathbf{q}\cdot\mathbf{r}_h}|\alpha,i\rangle\ , \tag{12}$$

$a_0$ being the lattice constant, $u_0$ the phonon zero-point amplitude of the relative sublattice displacement,[10] and $D_\alpha(\mathbf{r}_\alpha)$ ($\alpha=e$ for the electron and $h$ for the hole) the deformation-potential constant as defined by Bir and Pikus.[19] In our three-band model the deformation-potential interaction can only act between different valence bands. The matrix element $\langle c|D_e(\mathbf{r}_e)|c\rangle\equiv 0$. Thus, in the Raman process, the electron in the conduction band does not change its quantum numbers via electron-phonon interaction. Furthermore, using the wave function (5) and Eq. (12) it is possible to show that

$$\langle\mu_j|H_{E\text{-}P}|\mu_i\rangle=\delta_{\mathbf{k}_e,\mathbf{k}_e'}\delta_{n_e,n_e'}\delta_{\mathbf{k}_n',\mathbf{k}_n-\mathbf{q}_\perp}$$
$$\times D_{v_i}^{v_j}e^{-iq_x x_{0h}}f_{n_h,n_h'}(q_x,q_y)\ , \tag{13}$$

where $D_{v_i}^{v_j}=\langle v_j|D_h(\mathbf{r}_h)|v_i\rangle$, $x_{0h}=-\lambda^2k_{hy}$; $\lambda=(\hbar c/eH)^{1/2}$ is the cyclotron radius, and

$$f_{n_h,n_h'}(q_x,q_y)=\int_{-\infty}^{\infty}dx\ \Phi_{n_h}(x)e^{iq_x x}$$
$$\times\Phi_{n_h'}\left[x+\frac{\hbar cq_y}{eH}\right]\ . \tag{14}$$

Introducing expressions (7), (11), and (13) into Eq. (10) and only keeping the term which dominates near resonance, the scattering amplitude can be written as

$$W_{\mathrm{FI}}=-\frac{\pi e^2\hbar}{m_0^2}\frac{\langle c|\mathbf{e}_s^*\cdot\mathbf{p}|v_j\rangle D_{v_i}^{v_j}\langle v_i|\mathbf{e}_l\cdot\mathbf{p}|c\rangle}{Vn_sn_l(\omega_s\omega_l)^{1/2}}\frac{u_0\sqrt{3}}{a_0}\sum_{\mathbf{k},n}\frac{e^{-iq_x x_{0h}}f_{n,n}(q_x,q_y)\delta_{q_z,0}\delta_{q_y,0}}{\left[\frac{\hbar^2k_z^2}{2\mu_i}+\hbar\omega_c^{(i)}(n+\frac{1}{2}-\beta_{li})\right]\left[\frac{\hbar^2k_z^2}{2\mu_j}+\hbar\omega_c^{(j)}(n+\frac{1}{2}-\beta_{sj})\right]} \tag{15}$$

where

$$\beta_{l(s)k}=\frac{\hbar\omega_{l(s)}-E_{g_k}-\mu_B H(g_e^*-g_{h_k}^*)m_{se}+i\Gamma_k}{\hbar\omega_c^{(k)}},\quad k=i,j \tag{16}$$

with $\omega_c^{(k)}=eH/\mu_k c$ and $\mu_k$ the reduced effective mass. In Eq. (15) we have taken $\kappa_l \approx \kappa_s \approx 0$ and made use of spin conservation. The Bose-Einstien phonon population factor was neglected because we consider only Stokes Raman scattering at low temperatures. Using the fact that $\sum_{k_y} \exp(-iq_x x_0)=(V^{2/3}/2\pi\lambda^2)\delta_{q_x,0}$ and integrating over $k_z$ in Eq. (15), we find that the scattering amplitude of a Raman process where the hole is scattered from valence band $i$ to $j$ is given by

$$W_{\mathrm{FI}}(i\rightarrow j)=I_0 R_{\mathrm{DP}}(\beta_{li},\beta_{sj}) , \tag{17}$$

where

$$R_{\mathrm{DP}}(\beta_{li},\beta_{sj})=\frac{\mu_B H R_H}{\hbar\omega_c^{(i)}\hbar\omega_c^{(j)}}\frac{a_H}{\lambda}\sum_{n=0}^{\infty}\frac{(\beta_{li}-n-\frac{1}{2})^{-1/2}-(\beta_{sj}-n-\frac{1}{2})^{-1/2}}{\beta_{li}-\beta_{sj}} \tag{18}$$

and

$$I_0=-\frac{i\sqrt{2}}{n_s n_l}\frac{\langle c|\mathbf{e}_s^*\cdot\mathbf{p}|v_i\rangle D_{v_i}^{v_j}\langle v_j|\mathbf{e}_l\cdot\mathbf{p}|c\rangle}{(\hbar\omega_l\hbar\omega_s)^{1/2}}\frac{u_0\sqrt{3}}{m_0 a_0} \tag{19}$$

with $a_H$ and $R_H$ being the hydrogen Bohr radius and Rydberg, respectively.

The above result differs from the scattering amplitude obtained in Ref. 16 in the denominator $\beta_{li}$-$\beta_{sj}$, which appears on the right-hand side of Eq. (18), and in the two, in general, different gaps $E_{g_k}$ and lifetime broadenings $\Gamma_k$ introduced in Eq. (16). This is due to the fact that a simple parabolic two-band model is considered in Ref. 16, while we are dealing with a three-band model. It can be seen from Eq. (18) that the scattering amplitude is proportional to $H$. As in Ref. 11, the limit $H\rightarrow 0$ can be obtained from Eq. (18) for the uncorrelated electron-hole scattering amplitude. Finally, the Raman efficiency of a process involving the transition $v_i\rightarrow v_j$ is given by

$$\frac{dS(i\rightarrow j)}{d\Omega}=S_{\mathrm{DP}}|R_{\mathrm{DP}}(\beta_{li},\beta_{sj})|^2 , \tag{20}$$

$$S_{\mathrm{DP}}=\left[\frac{\omega_s}{\omega_l}\right]^2\frac{n_s}{n_l}\frac{Vu_0^2}{2\pi^2 a_0^2 c^4\hbar^4 m_0^2}\times|\langle c|\mathbf{e}_s^*\cdot\mathbf{p}|v_j\rangle D_{v_i}^{v_j}\langle v_i|\mathbf{e}_l\cdot\mathbf{p}|c\rangle|^2 . \tag{21}$$

### A. Selection rules

We consider the case of backscattering from a (001) surface of a cubic semiconductor in Faraday configuration ($\mathbf{H}\|+\hat{\mathbf{z}},\mathbf{k}_{\mathrm{light}}\|\mp\mathbf{H}$). In this case, the matrix representation of $D_h$ is[20]

$$D_h=d_0\begin{bmatrix}0&1&0\\1&0&0\\0&0&0\end{bmatrix} , \tag{22}$$

where $d_0$ is the optical deformation-potential constant. In III-V compounds, in the vicinity of the $E_0$ and $E_0+\Delta_0$ critical points, different transitions between the conduction band and the three valence bands, corresponding to heavy (hh), light (lh), and spin-orbit split-off (so) holes, will contribute to the resonances [see Fig. 1(a)]. The valence-band wave functions $|J,J_z\rangle$, where $J$ is the total angular momentum and $J_z$ its $z$ component ($J=\frac{3}{2}$ for $\Gamma_8^v$ and $J=\frac{1}{2}$ for $\Gamma_6^c$ and $\Gamma_7^s$), can be represented as[21]

$$\begin{aligned}
v_{\mathrm{hh}}^{+}&=|\tfrac{3}{2},+\tfrac{3}{2}\rangle=\frac{1}{\sqrt{2}}|(X+iY)\uparrow\rangle ,\\
v_{\mathrm{hh}}^{-}&=|\tfrac{3}{2},-\tfrac{3}{2}\rangle=\frac{1}{\sqrt{2}}|(X-iY)\downarrow\rangle ,\\
v_{\mathrm{lh}}^{+}&=|\tfrac{3}{2},+\tfrac{1}{2}\rangle=\frac{1}{\sqrt{6}}|(X+iY)\downarrow-2Z\uparrow\rangle ,\\
v_{\mathrm{lh}}^{-}&=|\tfrac{3}{2},-\tfrac{1}{2}\rangle=\frac{1}{\sqrt{6}}|(X-iY)\uparrow+2Z\downarrow\rangle ,\\
v_{\mathrm{so}}^{+}&=|\tfrac{1}{2},+\tfrac{1}{2}\rangle=\frac{1}{\sqrt{3}}|(X+iY)\downarrow+Z\uparrow\rangle ,\\
v_{\mathrm{so}}^{-}&=|\tfrac{1}{2},-\tfrac{1}{2}\rangle=\frac{1}{\sqrt{3}}|(X-iY)\uparrow-Z\downarrow\rangle ,
\end{aligned} \tag{23}$$

where the [001] direction has been chosen as the quantization axis. The wave functions for the conduction band $|c\rangle$ are $|S\uparrow\rangle$ and $|S\downarrow\rangle$.

For circularly polarized light [$\mathbf{e}_{\pm}=\sigma^{\pm}=(\mathbf{e}_x\pm i\mathbf{e}_y)/\sqrt{2}$] Raman processes mediated by deformation-potential electron-phonon interaction are possible in two scattering configurations: $\bar{z}(+,-)z$ or $\bar{z}(-,+)z$. It immediately follows from Eqs. (22) and (23) that there are no processes allowed by this mechanism in the $\bar{z}(\pm,\pm)z$ configurations.

Table I(a) shows the nonzero matrix elements $\langle c|\mathbf{e}_{\pm}^*\cdot\mathbf{p}|v_j\rangle D_{v_i}^{v_j}\langle v_i|\mathbf{e}_{\mp}\cdot\mathbf{p}|c\rangle$ for the different diagrams which contribute to resonant Raman scattering in the region of the $E_0$ and $E_0+\Delta_0$ gaps. It can be seen that via deformation potential the spin-orbit valence band $|\frac{1}{2},\pm\frac{1}{2}\rangle$ can only be connected with the heavy-hole valence band $|\frac{3}{2},\mp\frac{3}{2}\rangle$. The light-hole states $|\frac{3}{2},\pm\frac{1}{2}\rangle$ couple with the $|\frac{3}{2},\mp\frac{3}{2}\rangle$ heavy-hole states. Furthermore, conduction-band states with spin up and down are both involved in Raman processes for each configuration.

The following selection rules for deformation-potential scattering are obtained:

$$\begin{aligned}
&\Delta J=0,\pm 1 ,\\
&\Delta m_s=m_{se}-m_{sh}=0 ,\\
&\Delta n=0 ,\\
&\Delta J_z=J_{zi}-J_{zj}=2 \quad \text{for } \bar{z}(-,+)z ,
\end{aligned} \tag{24}$$

and

$$\Delta J_z=-2 \quad \text{for } \bar{z}(+,-)z .$$

TABLE I. Values of (a) $\langle c|\mathbf{e}_{\pm}^{*}\cdot\mathbf{p}|v_j\rangle D_{v_i}^{v_j}\langle v_i|\mathbf{e}_{\mp}\cdot\mathbf{p}|c\rangle$ and (b) $\langle c|\mathbf{e}_{\pm}^{*}\cdot\mathbf{p}|v_i\rangle\ \langle v_i|\mathbf{e}_{\pm}\cdot\mathbf{p}|c\rangle$ for the different transitions involved in the vicinity of $E_0$ and $E_0+\Delta_0$ critical points. ↑ (↓) denote spin up (down) of the conduction-band wave functions involved in the respective Raman processes.

(a) $\langle c|\mathbf{e}_{\pm}^{*}\cdot\mathbf{p}|v_j\rangle D_{v_i}^{v_j}\langle v_i|\mathbf{e}_{\mp}\cdot\mathbf{p}|c\rangle$

| transition | $\bar{z}(-,+)z$ | transition | $\bar{z}(+,-)z$ |
|---|---|---|---|
| $v_{hh}^{+}\rightarrow v_{lh}^{-}$ | $i\frac{\lvert P\rvert^2}{3}d_0$ (↑) | $v_{hh}^{-}\rightarrow v_{lh}^{+}$ | $-i\frac{\lvert P\rvert^2}{3}d_0$ (↓) |
| $v_{lh}^{+}\rightarrow v_{hh}^{-}$ | $i\frac{\lvert P\rvert^2}{3}d_0$ (↓) | $v_{lh}^{-}\rightarrow v_{hh}^{+}$ | $-i\frac{\lvert P\rvert^2}{3}d_0$ (↑) |
| $v_{so}^{+}\rightarrow v_{hh}^{-}$ | $i\frac{2\lvert P\rvert^2}{3}d_0$ (↓) | $v_{so}^{-}\rightarrow v_{hh}^{+}$ | $-i\frac{2\lvert P\rvert^2}{3}d_0$ (↑) |
| $v_{hh}^{+}\rightarrow v_{so}^{-}$ | $i\frac{2\lvert P\rvert^2}{3}d_0$ (↑) | $v_{hh}^{-}\rightarrow v_{so}^{+}$ | $-i\frac{2\lvert P\rvert^2}{3}d_0$ (↓) |

(b) $\langle c|\mathbf{e}_{\pm}^{*}\cdot\mathbf{p}|v_i\rangle\langle v_i|\mathbf{e}_{\pm}\cdot\mathbf{p}|c\rangle$

| transition | $\bar{z}(-,-)z$ | transition | $\bar{z}(+,+)z$ |
|---|---|---|---|
| $v_{hh}^{+}\rightarrow v_{hh}^{+}$ | $\lvert P\rvert^2$ (↑) | $v_{hh}^{-}\rightarrow v_{hh}^{-}$ | $\lvert P\rvert^2$ (↓) |
| $v_{lh}^{+}\rightarrow v_{lh}^{+}$ | $\frac{\lvert P\rvert^2}{3}$ (↓) | $v_{lh}^{-}\rightarrow v_{lh}^{-}$ | $\frac{\lvert P\rvert^2}{3}$ (↑) |
| $v_{so}^{+}\rightarrow v_{so}^{+}$ | $\frac{2\lvert P\rvert^2}{3}$ (↓) | $v_{so}^{-}\rightarrow v_{so}^{-}$ | $\frac{2\lvert P\rvert^2}{3}$ (↑) |

For dipole-allowed interband magneto-optical transitions the usual selection rules $\Delta n=0$, $\Delta J_z=\pm 1$ for $\sigma^{\pm}$ polarized light are used. Using these selection rules and the results of Table I(a) it is possible to obtain the total Raman efficiency by adding the different contributions coherently. In the $\bar{z}(-,+)z$ configuration, for example, we have

$$\frac{dS}{d\Omega}=S_{DP}(v_{so}^{+}\rightarrow v_{hh}^{-})\left|\tfrac{1}{2}R_{DP}(v_{hh}^{+}\rightarrow v_{lh}^{-})+\tfrac{1}{2}R_{DP}(v_{lh}^{+}\rightarrow v_{hh}^{-})+R_{DP}(v_{so}^{+}\rightarrow v_{hh}^{-})+R_{DP}(v_{hh}^{+}\rightarrow v_{so}^{-})\right|^2 . \quad (25)$$

Figure 1(a) schematically shows the Landau levels as a function of the magnetic field for the $\Gamma_6^c$, $\Gamma_8^v$, and $\Gamma_7^s$ bands. The different interband magneto-optical transitions and the transitions mediated by deformation-potential interaction for the $\bar{z}(+,-)z$ and $\bar{z}(-,+)z$ scattering configurations are presented in Fig. 1(b). As can be seen in Fig. 1, no valence-band mixing has been considered in the simple parabolic three-band model studied here. If the valence-band mixing is taken into account, the magnetic levels have admixtures of Landau states which differ in the quantum number $n$,[5–7] but the selection rules for $J,J_z$ and the spin remain. Furthermore, the selection rules $\Delta J_z=\pm 2$ cause differences between the spectra in the two scattering configurations with opposite circular polarizations. For example, let us consider the resonant so→hh valence-band transitions: In the $\bar{z}(-,+)z$ configuration the Raman process couples via a spin-down conduction-band level with scattering of the hole between $v_{so}^{+}$ and $v_{hh}^{-}$ states, whereas in $\bar{z}(+,-)z$ a spin-up state and the $v_{so}^{-}$ and $v_{hh}^{+}$ states are involved. The electron and hole $g$ factors lead to a difference in the interband transition energies for the two processes which is given by

$$\Delta E=\mu_B H(g_e^{*}-g_{h_j}^{*}) . \quad (26)$$

For fixed laser energies the difference in magnetic field of incoming (outgoing) resonances involving levels with the same Landau $n$ but occurring in the two complementary configurations is

$$\Delta H_n=\frac{(\hbar\omega_{l(s)}-E_{g_j})(g_e^{*}-g_{h_j}^{*})}{\mu_B\left[\left[\frac{m_0}{\mu_j}(2n+1)\right]^2-\left[\frac{g_e^{*}-g_{h_j}^{*}}{2}\right]^2\right]} . \quad (27)$$

$\Delta E$ is independent of $n$ while $\Delta H_n$ decreases like $(2n)^{-2}$. If the spin quantization can be neglected or if $g_e^{*}\approx g_{h_j}^{*}$, the same behavior of the Raman efficiency as a function of $\hbar\omega_l$ or $H$ should be observed for both configurations.

### B. Double-resonance condition

When the incident and scattered light are simultaneously in resonance with electronic interband transitions, the conditions for doubly resonant first-order Raman scattering (DRRS) are fulfilled. The condition for DRRS, which is that the difference in energy between two electronic transitions must be equal to the energy $\hbar\omega_0$ of the phonon under consideration, has been obtained previously by several methods: choosing the appropriate thickness of a quantum-well structure,[22] applying an electric field,[23] or a uniaxial stress.[24] Experimental and theoretical evidence for magnetic-field-induced double resonance was found in the course of this work.[25,26] The presence of an external magnetic field splits the $\Gamma_6^c$, $\Gamma_8^v$, and $\Gamma_7^s$ bands into singlets [see Fig. 1(a)]. A suitable magnetic field can induce an energy splitting equal to $\hbar\omega_0$. Assuming that the incident light is in resonance with an interband magneto-optical electronic transition

from one of the valence bands to the conduction band, and that the scattered light is in resonance with a transition from another valence band to the same conduction band, the condition for double resonance will thus be fulfilled when the two valence levels can couple via deformation-potential electron-phonon interaction. The double-resonance condition can be obtained using Eqs. (16) and (18). It follows that the critical magnetic field $H_n^{\mathrm{DR}}$ is given by

$$H_n^{\mathrm{DR}}=\frac{\hbar\omega_0-E_{g_i}+E_{g_j}}{\mu_B\left[\dfrac{m_0}{m_i^*}-\dfrac{m_0}{m_j^*}\right](2n+1)-\mu_B(g_{h_i}^*-g_{h_j}^*)m_{s_e}} \tag{28}$$

and the laser frequency for which the double resonance occurs is equal to

$$\hbar\omega_l^{\mathrm{DR}}=E_{g_i}+\hbar\omega_c^{(i)}(H_n^{\mathrm{DR}})(n+\tfrac{1}{2})+\mu_B H_n^{\mathrm{DR}}(g_e^*-g_{h_i}^*)m_{s_e}\ . \tag{29}$$

Figure 2 shows the Raman efficiency due to the $v_{\mathrm{lh}}^- \rightarrow v_{\mathrm{hh}}^+$ term in the $\bar{z}(+,-)z$ configuration for laser energies below and above the DRRS condition as a function of the magnetic field. In the calculation parameters for GaAs were used. The effective band parameters $m^*, g^*$ were evaluated using the expressions from Ref. 27 and they are summarized in Table II. For an incident laser energy of $\hbar\omega_l = 1.61$ eV one recognizes the typical oscillations of the intensity due to incoming and outgoing resonances for different Landau quantum numbers $n$ as a function of the applied magnetic field. The incoming resonances (dashed arrows) correspond to light-hole–to–conduction-band magneto-optical transitions while the outgoing ones (solid arrows) are due to transitions between the conduction and heavy-hole Landau levels. According to Eq. (20) the Raman efficiency should increase like $H^2$. The ratio between $\Gamma_{e\text{-hh}}$ and $\Gamma_{e\text{-lh}}$ determines the relative strength of the incoming and outgoing resonances. As the laser energy is increased the incoming and outgoing resonances for each $n$ move closer towards each other. For $\hbar\omega_l \approx 1.63$ eV the resonances of the incoming and scattered light coincide at the DRRS critical magnetic fields $H_n^{\mathrm{DR}}$ and a maximum in the Raman intensity is obtained. The denominators in the expression for the Raman efficiency vanish except for the lifetime broadenings. In this case the phonon intensity clearly shows the parabolic dependence on the magnetic field mentioned above. Due to the small value of $\mu_B H(g_{h_i}^* - g_{h_j}^*)m_{s_e}$ compared to the cyclotron energies, the critical laser energies are practically independent of the Landau quantum number $n$. Neglecting the $g$-factor contributions one obtains

$$\hbar\omega_l^{\mathrm{DR}} \approx E_g + \frac{m_{\mathrm{hh}}^*}{m_e^*}\,\frac{m_e^*+m_{\mathrm{lh}}^*}{m_{\mathrm{hh}}^*-m_{\mathrm{lh}}^*}\hbar\omega_0\ , \tag{30}$$

which gives $\hbar\omega_l^{\mathrm{DR}} \approx 1621$ meV using the parameters of Table II. For laser energies above $\hbar\omega_l^{\mathrm{DR}}$, the incoming resonance for the same $n$ occurs at lower magnetic fields than the outgoing resonance, whereas the reverse is true for laser energies below $\hbar\omega_l^{\mathrm{DR}}$. This clearly demonstrates that magnetic-field-induced DRRS is obtained when the two magneto-optical transitions differ by the energy of a phonon and the lh→hh transition is mediated by deformation-potential electron-phonon interaction.

TABLE II. Parameters used for the evaluation of the Raman efficiency near the double resonance condition in GaAs (Fig. 2).

| | | |
|---|---|---|
| $E_0 = 1519$ meV[a] | $\Delta_0 = 341$ meV[a] | $\hbar\omega_0 = 37$ meV[a] |
| $m_e^* = 0.068 m_0$[b] | $g_e^* = -0.32$[c] | |
| $m_{\mathrm{hh}}^* = 0.491 m_0$[c] | $g_{\mathrm{hh}}^* = -4.5$[c] | $\Gamma_{e\text{-hh}} = 1$ meV |
| $m_{\mathrm{lh}}^* = 0.086 m_0$[c] | $g_{lh}^* = 18.1$[c] | $\Gamma_{e\text{-lh}} = 3$ meV |
| $m_{\mathrm{so}}^* = 0.176 m_0$[c] | $g_{\mathrm{so}}^* = 4.5$[c] | $\Gamma_{e\text{-so}} = 10$ meV |

[a]Reference 31.
[b]Reference 32.
[c]Calculated from Luttinger parameters given in Ref. 27.

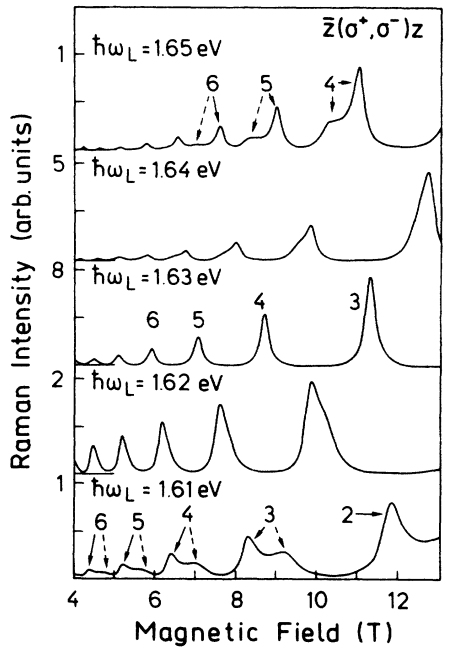


FIG. 2. Raman intensity as a function of the magnetic field for laser energies near the double resonance condition in $\bar{z}(+,-)z$ configuration. For clarity only the $v_{\mathrm{lh}}^- \rightarrow v_{\mathrm{hh}}^+$ term is shown. The parameters used in the calculation are typical for GaAs (see Table II). Dashed arrows label the incoming resonances while the solid arrows point to the outgoing resonances for Landau quantum numbers $n$.

## IV. DIPOLE-FORBIDDEN FRÖHLICH INTERACTION

The coupling constant for the interaction between electrons and long-wavelength LO phonons (Fröhlich interaction) is[17]

$$S^{\alpha',j}_{\alpha,i}(\mathbf{q})=\frac{C_F}{|\mathbf{q}|}\langle\alpha',j|e^{i\mathbf{q}\cdot\mathbf{r}_e}-e^{i\mathbf{q}\cdot\mathbf{r}_h}|\alpha,i\rangle\ , \tag{31}$$

$$C_F=-i(\epsilon_\infty^{-1}-\epsilon_0^{-1})^{1/2}(2\pi e^2\hbar\omega_0/V)^{1/2}\ , \tag{32}$$

$\epsilon_0$ being the static and $\epsilon_\infty$ the optical dielectric constants. Introducing expression (5) into Eq. (31) the matrix element $\langle\mu_2|H_{E\text{-}P}|\mu_1\rangle$ can be written as

$$\langle\mu_2|H_{E\text{-}P}|\mu_1\rangle=(\delta_{\mathbf{k}'_h,\mathbf{k}_h}\delta_{\mathbf{k}'_e,\mathbf{k}_e-\mathbf{q}_\perp}\delta_{n'_e,n_e}e^{-iq_xx'_{0_e}}-\delta_{\mathbf{k}'_e,\mathbf{k}_e}\delta_{\mathbf{k}'_h,\mathbf{k}_h-\mathbf{q}_\perp}\delta_{n'_h,n_h}e^{-iq_xx'_{0_h}})\times\frac{C_F^*}{|\mathbf{q}|}f_{n_e,n_e}(q_x,q_y)\ . \tag{33}$$

Using expressions (7), (11), and the above matrix element, the scattering amplitude becomes

$$W_{\mathrm{FI}}=A_0R_F(\beta_{lj},\beta_{sj})\ , \tag{34}$$

where

$$R_F(\beta_{lj},\beta_{sj})=\frac{\mu_BH\,R_H}{(\hbar\omega_c^{(j)})^2}\left[\frac{m^*_{h_j}-m_e^*}{m^*_{h_j}+m_e^*}\right]\frac{a_H}{\lambda}\sum_{n=0}^{\infty}\frac{[(\beta_{lj}-n-\frac{1}{2})^{1/2}+(\beta_{sj}-n-\frac{1}{2})^{1/2}]^{-3}}{[(\beta_{lj}-n-\frac{1}{2})(\beta sj-n-\frac{1}{2})]^{1/2}}\ , \tag{35}$$

$$A_0=-i\sqrt{2}\frac{\langle c|\mathbf{e}_s^*\cdot\mathbf{p}|v_j\rangle\langle v_j|\mathbf{e}_l\cdot\mathbf{p}|c\rangle}{n_sn_lm_0(\hbar\omega_l\hbar\omega_s)^{1/2}}\frac{|C_F|}{q}(\lambda q_z)^2\ . \tag{36}$$

Since the wave vector of phonons being involved in the one-phonon RRS is very small, we only include terms proportional to $q^2$ in Eq. (34) and $f_{n,n}(q_x,q_y)$ is approximated by 1. The fact that $H_{E\text{-}P}$ may couple only intraband and intralevel has already been considered in these equations. The limit $H\rightarrow0$ can be recovered from Eq. (34) by substituting

$$y_n=\hbar\omega_c^{(j)}(n+\tfrac{1}{2}) \tag{37}$$

and converting the summation $\sum_n$ into $1/\hbar\omega_c^{(j)}\int_0^\infty dy$. After evaluating the integral the well known uncorrelated electron-hole model for the Fröhlich interaction is obtained:[18,28]

$$W_{\mathrm{FI}}=-i\frac{\sqrt{2}}{3}\left[\frac{\mu_j}{m_0}\right]^{1/2}\left[\frac{m^*_{h_j}-m_e^*}{m^*_{h_j}+m_e^*}\right]A_0\left[\frac{R_H}{\hbar\omega_0}\right]^{1/2}\times\frac{\hbar^2}{2m_0\lambda^2}\frac{1}{\hbar\omega_0}\left[\left[\frac{\hbar\omega_l-E_g+i\Gamma}{\hbar\omega_0}\right]^{1/2}-\left[\frac{\hbar\omega_s-E_g+i\Gamma}{\hbar\omega_0}\right]^{1/2}\right]^3\ . \tag{38}$$

As in the deformation-potential case the scattering amplitude is proportional to the magnetic field. The Raman intensity is given by the expression

$$\frac{dS(j\rightarrow j)}{d\Omega}=S_F|R_F(\beta_{lj},\beta_{sj})|^2 \tag{39}$$

$$S_F=\left[\frac{\omega_s}{\omega_l}\right]^2\frac{n_s}{n_l}\frac{V}{2\pi^2c^4\hbar^4m_0^2}\frac{|C_F|^2}{q^2}(\lambda q_z)^4\times|\langle c|\mathbf{e}_s^*\cdot\mathbf{p}|v_j\rangle\langle v_j|\mathbf{e}_l\cdot\mathbf{p}|c\rangle|^2\ . \tag{40}$$

Unlike in the case of deformation-potential interaction, DRRS cannot be achieved with dipole-forbidden Fröhlich interaction in the framework of this simple band model. Defining the scattering configurations as in Sec. III and using the wave functions given in Eq. (23), the selection rule $\Delta J=0$, $\Delta J_z=0$, $\Delta m_s=0$, and $\Delta n=0$ is obtained, which allows for scattering in the $\bar{z}(\pm,\pm)z$ configurations. The $\bar{z}(\pm,\mp)z$ configurations are forbidden. The nonzero values of $\langle c|\mathbf{e}_\pm^*\cdot\mathbf{p}|v_j\rangle\langle v_j|\mathbf{e}_\pm\cdot\mathbf{p}|c\rangle$ for the $E_0$ and $E_0+\Delta_0$ critical points are given in Table I(b). The different interband magneto-optical transitions, the Landau levels, and the transitions mediated by Fröhlich interaction for the $\bar{z}(\pm,\pm)z$ configurations are shown in Fig. 1(c). For the $\bar{z}(\sigma^+,\sigma^+)z$ configuration, for example, the total Raman efficiency is given by

$$\frac{dS}{d\Omega}=S_F(v_{\mathrm{hh}}^-\rightarrow v_{\mathrm{hh}}^-)|R_F(v_{\mathrm{hh}}^-\rightarrow v_{\mathrm{hh}}^-)+\tfrac{1}{3}R_F(v_{\mathrm{lh}}^-\rightarrow v_{\mathrm{lh}}^-)+\tfrac{2}{3}R_F(v_{\mathrm{so}}^-\rightarrow v_{\mathrm{so}}^-)|^2\ . \tag{41}$$

As a function of $\hbar\omega_l$ or $H$ the Raman intensity shows a series of resonances for the incident and scattered light whenever $\hbar\omega_{l(s)}=E_{g_j}+\hbar\omega_c^{(j)}(n+\frac{1}{2})+\mu_BH(g_e^*-g^*_{h_i})m_{s_e}$. From Eq. (39) and Fig. 1 it can be understood that the resonances for the same Landau quantum number $n$ occur at different magnetic fields or laser energies for the two scattering configurations $\bar{z}(\pm,\pm)z$, a fact which is due to the $g$-factor splitting. As in the deformation-potential case, the energy separation $\Delta E$ (for constant $H$) and $\Delta H$ (for constant energy) between two peaks originating from the same Landau $n$ in the two types of spectra are given by Eqs. (26) and (27), respectively.

## V. ADAPTATION TO A REALISTIC BAND STRUCTURE AND COMPARISON WITH EXPERIMENT

In the attempt to fit the theory just developed to experimental results it is found that the parabolic three-brand model is only a rough approximation for the complex features which are observed experimentally. As is well known, the valence levels of cubic semiconductors in a

magnetic field are not pure product states of Bloch and oscillator wave functions. Diagonalization of an $8\times8$ $\mathbf{k}\cdot\mathbf{p}$ Hamiltonian yields rather a sum of these basis functions which may be admixed to a considerable degree.[6-8]

Since, however, our theory was developed for general basis product functions [Eq. (5)] it can easily be adapted to any sophisticated wave functions obtained from the more accurate Hamiltonians. This is accomplished by applying the selection rules found in Secs. III and IV and multiplying with the corresponding weight coefficients. The Landau ladders are in general not going to be equidistant any more, especially for small oscillator quantum numbers $n$ where quantum effects become evident. This can readily be taken into account within the framework of our theory by simply converting the magnetic energies into effective masses according to $E=(e\hbar H/m^*c)(n+\frac{1}{2})$. Thus the effective mass is no longer treated as a constant but rather as a function of Landau $n$ and magnetic field $H$. The nonparabolicity of the conduction band can be incorporated in the same way and corrections due to Coulomb interaction between electrons and holes may be treated as a renormalization of the levels. A step away from the parabolic model towards a more realistic band structure in a magnetic field was given in the work of Luttinger and Kohn.[5,6] In the approximation $k_z=0$, which is justified by the divergence of the one-dimensional density of states and the low temperatures at which these experiments are usually performed, the $8\times8$ $\mathbf{k}\cdot\mathbf{p}$ Hamiltonian can be separated into two $2\times2$ blocks for the $\Gamma_8^v$ valence bands and be solved analytically. Admixed wave functions

$$\begin{aligned}\Psi_1^{\pm}&=a_1^{\pm}|n-2,\tfrac{3}{2},+\tfrac{3}{2}\rangle+a_2^{\pm}|n,\tfrac{3}{2},-\tfrac{1}{2}\rangle\ ,\\ \Psi_2^{\pm}&=b_1^{\pm}|n-2,\tfrac{3}{2},+\tfrac{1}{2}\rangle+b_2^{\pm}|n,\tfrac{3}{2},-\tfrac{3}{2}\rangle\ ,\end{aligned}\tag{42}$$

are obtained for the eigenvalues $E(1-)$, $E(2-)$ for heavy-mass ladders and $E(1+)$, $E(2+)$ for light-mass ladders. When dealing with these solutions the assignment of single $|n,J,J_z\rangle$ states to heavy- or light-hole levels becomes meaningless. The terminology of heavy- or light-mass levels should rather be used in order to characterize the narrow or widely spaced ladders which consist of admixtures of both heavy- and light-hole states of the simple three-band parabolic model. The valence-level structure resulting from this extension is schematically presented in Fig. 3. The parameters used to describe these levels are the Luttinger parameters[5,6,26] and $g$-factor splittings are now implicity incorporated in the diagonalization of the $2\times2$ blocks, which couple oscillator functions differing by $\Delta n=2$.

A comparison of the energy levels calculated with Luttinger's formulae to the more precise theory by Trebin *et al.*[8] gives good agreement for the heavy-mass levels, whereas the light-mass ones show differences of more than 5 meV for $n>5$. However, the admixing factors obtained from both theories are pretty similar and the comparison suggests that the approximation of the valence levels by the analytical results is valid for GaAs. In the case of InP, however, the wave functions are found to be dominated by three or even four admixtures[3] and thus this approximation is probably not too realistic.

Maintaining the parabolic approximation for the conduction and split-off levels, and using the $\Gamma_8^v$ valence-level structure just described, additional Raman processes become possible which are shown in Fig. 3. While leaving the detailed discussion of the consequences of this extension to the following paper[26] we note that due to the valence-level mixing there are now also channels for magnetic-field-induced double resonances with Fröhlich-interaction-mediated processes observable in $\bar{z}(\pm,\pm)z$. This is possible because states $|n,J,J_z\rangle$, which participate in intraband and intralevel Fröhlich coupling, are now admixtures of both heavy- and light-mass levels. A problem is, however, still left. While the $|\frac{3}{2},\pm\frac{3}{2}\rangle$ components of the light- and heavy-mass eigenstates now couple via Fröhlich interaction, so do the corresponding $|\frac{3}{2},\pm\frac{1}{2}\rangle$ components. Orthogonality makes the total coupling again equal to zero. In what follows we nevertheless treat this coupling as nonvanishing, a fact that can be easily justified if the in-plane wave vector of the phonon is not zero.[9] In our backscattering configuration this can only be achieved through scattering by defects. A quantitative understanding of these problems requires further work. Under the assumptions just mentioned the coupling light- and heavy-mass levels can be split by a magnetic field to have a separation of one LO phonon leading to double resonance, whereas in the model discussed before they can only contribute to incoming or outgoing resonances. The results obtained by this approach are justified by our experiments.[25,26] Furthermore there are now two series of double resonances for each scattering configuration which involve phonon emission by scattering of holes between light- and heavy-mass levels.

A comparison of experimental spectra (solid lines) with the theory (dashed lines) for four different scattering configurations is given in Fig. 4. In the calculations all terms of Fig. 3 were considered. The parameters used to calculate the Landau levels are given in Ref. 26. The conduction-band nonparabolicity[1] and Coulomb corrections[3] were incorporated as just described. A term $b_1\cdot H+b_0$ ($b_1,b_0$ constant) was coherently added to the calculated spectra in order to phenomenologically describe the background that is found for increasing magnetic fields. We have some indications that this background is due to multiphonon scattering in the excitonic polariton regime.[29] The lifetime broadenings were chosen as a compromise between recent results[30] and the widths of the features that we observe in our spectra and taken as constants for all Landau $n$ and at all magnetic fields. This approximation is actually not valid since the rapid decreasing of the experimental features for larger $n$ supports the model that the lifetime of states becomes shorter the further they are away from the $E_0$ fundamental gap, which is due to acoustic-phonon emission. Due to the complications involved with a lifetime which depends on Landau $n$ and $H$, we decided to treat the linewidths as constants rather than to obtain a better fit at the expense of clarity.

As described in more detail in the following paper,[26] all the spectra of Fig. 4 except the one in the $\bar{z}(-,+)z$ configuration correspond to situations which are close to double resonance. In the spectra where Fröhlich scattering contributes, the phonon is emitted by coupling be-

tween the admixtures of $J_z=-\frac{1}{2}$ $[\bar{z}(+,+)z]$ and $J_z=+\frac{3}{2}$ $[\bar{z}(-,-)z]$ in the light- and heavy-mass levels. The resonances in the $\bar{z}(+,-)z$ spectrum where deformation-potential scattering occurs originate from couplings between $J_z=-\frac{1}{2}$ (in) to $J_z=+\frac{3}{2}$ (out) wave functions. The oscillator quantum number $n$ is conserved in our theory and is indicated in Fig. 4. The spectrum in $\bar{z}(-,+)z$ configuration is typical for a region remote

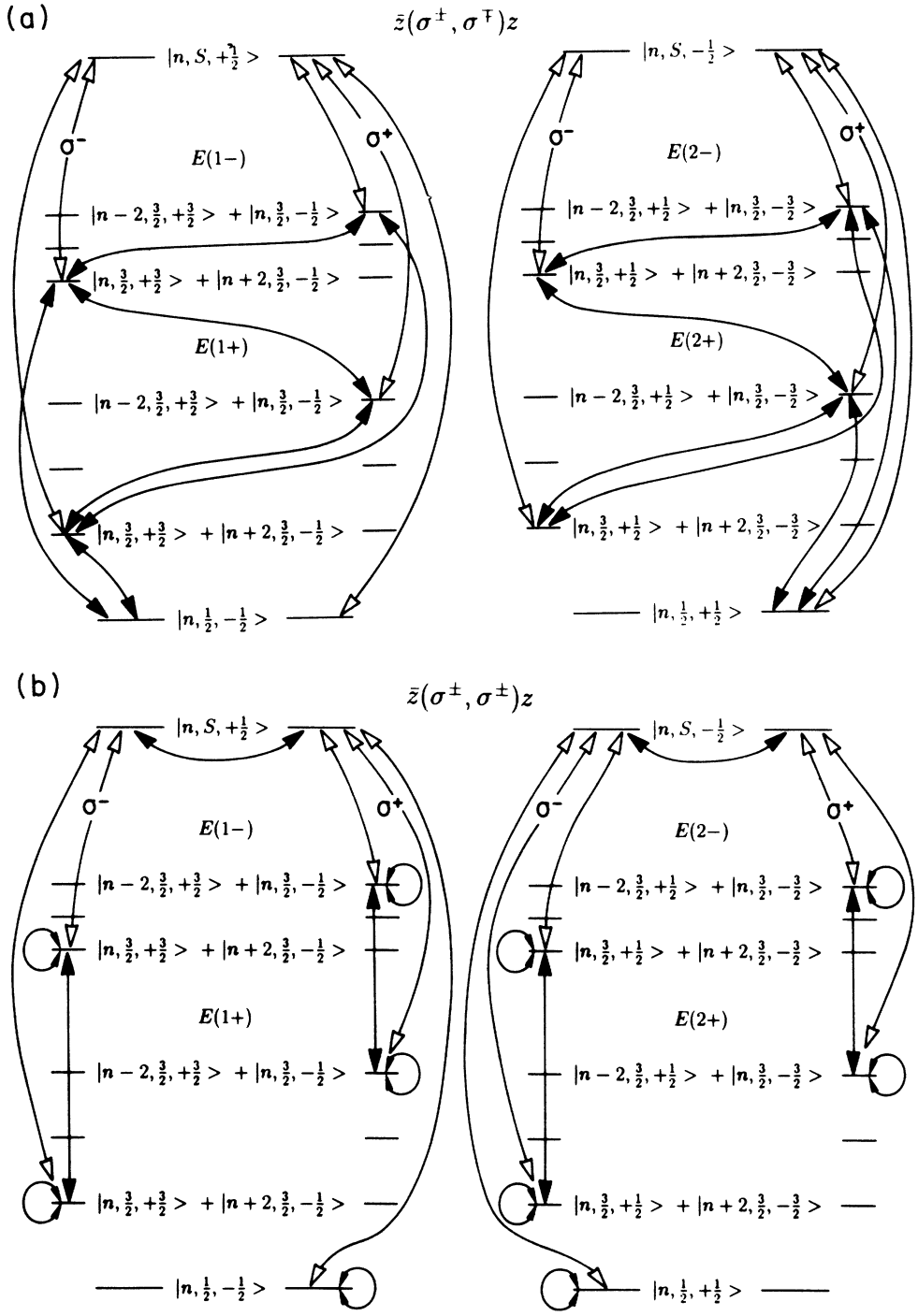


FIG. 3. Terms considered in the calculation of the Raman efficiency in a magnetic field using the Luttinger formulas for the mixed $\Gamma_8^v$ valence levels. (a) Transitions between Landau levels which contribute to Raman processes in the $\bar{z}(+,-)z$ and $\bar{z}(-,+)z$ scattering configurations: deformation-potential interaction. (b) Idem for the $\bar{z}(+,+)z$ and $\bar{z}(-,-)z$ scattering configurations: Fröhlich interaction. Open arrows represent interband magneto-optical transitions allowed in the Raman processes, solid arrows the transitions mediated by the electron-phonon interaction.

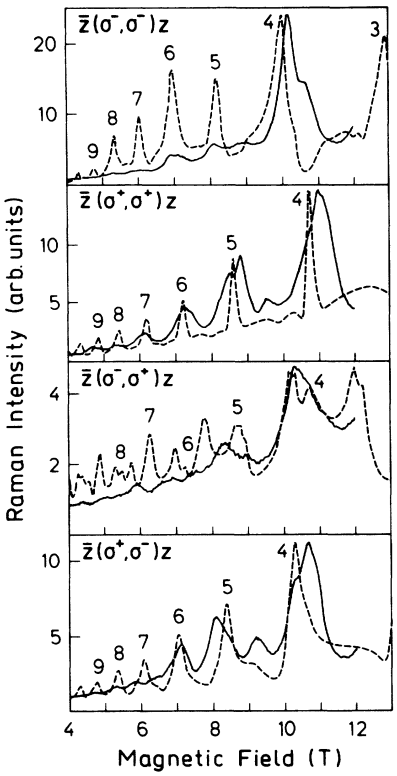


FIG. 4. Calculated Raman intensities (dashed lines) vs $H$ compared to magneto-Raman spectra of GaAs (solid lines) for an incident laser energy $\hbar\omega_l = 1.64$ eV in four different scattering configurations. The theoretical resonances are labeled with the respective Landau $n$. See text for details about the transitions.

from double resonance. There a multitude of incoming and outgoing resonances show up in the theoretical spectrum and a detailed analysis of each term separately is necessary to sort out the different contributions.

This comparison between experiment and theory, expanded in the following paper, shows that the theory developed in Secs. III and IV is an adequate model of resonant Raman scattering in a magnetic field. It can be used to describe the essential features of magneto-Raman experiments when adapted to a realistic band structure.

## VI. CONCLUSIONS

We have developed a theory of one-phonon resonant Raman scattering in a magnetic field in diamond- and zinc-blende-type semiconductors. Deformation potential and Fröhlich interactions were considered to mediate the electron–one-phonon coupling. Selection rules were obtained which show that the Raman tensor is not symmetric and that its components have different values for different scattering configurations: the dipole-allowed deformation-potential mechanism leads to coupling in $\bar{z}(+,-)z$ and $\bar{z}(-,+)z$, while the intrinsic dipole-forbidden Fröhlich interaction can be seen in $\bar{z}(+,+)z$ and $\bar{z}(-,-)z$. The nonsymmetric characteristic of the Raman tensor arises from the Landau-level spin splitting. The calculated Raman efficiencies exhibit strong oscillations as a function of laser energy or magnetic field which correspond to incoming or outgoing resonances with Landau levels. Conditions for magnetic-field-induced first-order doubly resonant Raman scattering by LO phonons were investigated. An extension of this theory was presented, which treats the $\Gamma_8^v$ valence levels in the framework of the Luttinger theory and takes into account additional terms which arise from valence level mixing. In this case double resonances may also occur in Fröhlich-interaction-mediated Raman processes which cannot be understood in a simple three-band model. As discussed in detail in the following paper agreement between this theory and the dominant features of the experimental spectra is found.

## ACKNOWLEDGMENTS

One of us (C.T.-G.) would like to acknowledge support from the Alexander von Humboldt Foundation (Bonn, Germany). We would also like to thank E. Burstein and G. LaRocca for a critical reading of the manuscript.

*Permanent address: Department of Theoretical Physics, Havana University, San Lázaro y L, Havana, Cuba.

[1]G. Ambrazevičius, M. Cardona, and R. Merlin, Phys. Rev. Lett. **59**, 700 (1987).

[2]T. Ruf, A. Cantarero, M. Cardona, J. Schmitz, and U. Rössler, in *Proceedings of the 19th International Conference on the Physics of Semiconductors,* edited by W. Zawadzki (Polish Academy of Sciences, Warsaw, 1988), p. 1473.

[3]T. Ruf, R. T. Phillips, A. Cantarero, G. Ambrazevičius, M. Cardona, J. Schmitz, and U. Rössler, Phys. Rev. B **39**, 13 378 (1989).

[4]M. Cardona, Surf. Sci. **37**, 100 (1973).

[5]J. M. Luttinger and W. Kohn, Phys. Rev. **97**, 869 (1955).

[6]J. M. Luttinger, Phys. Rev. **102**, 1030 (1956).

[7]C. R. Pidgeon and R. N. Brown, Phys. Rev. **146**, 575 (1966).

[8]H.-R. Trebin, U. Rössler, and R. Ranvaud, Phys. Rev. B **20**, 686 (1979).

[9]F. G. Bass and I. B. Levinson, Zh. Eksp. Teor. Fiz. **49**, 914 (1965) [Sov. Phys.—JETP **22**, 635 (1966)].

[10]O. A. Wolff, Phys. Rev. Lett. **16**, 225 (1966).

[11]Y. Yafet, Phys. Rev. **152**, 858 (1966).

[12]R. C. Enck, A. S. Saleh, and M. Y. Fan, Phys. Rev. **182**, 790 (1969).

[13]A. J. C. Sampaio and R. Luzzi, Phys. Status Solidi B **91**, 305 (1979).

[14]A. V. Gol'tsev, I. G. Lang, and S. T. Pavlov, Phys. Status Solidi B **91**, 305 (1979).

[15]F. Comas, C. Trallero-Giner, I. G. Lang, and S. T. Pavlov, Fiz. Tverd. Tela **27**, 57 (1985) [Sov. Phys.—Solid State **27**, 32 (1985)].

[16]R. Enderlein and F. Bechstedt, Phys. Status Solidi B **80**, 225 (1977).

[17]M. Cardona, in *Light Scattering in Solids II,* Vol. 50 of *Topics in Applied Physics,* edited by M. Cardona and G. Güntherodt (Springer, Heidelberg, 1982), p. 19.
[18]R. M. Martin, Phys. Rev. B **4**, 3676 (1971).
[19]G. E. Pikus and G. L. Bir, Fiz. Tverd. Tela **1**, 154 (1959) [Sov. Phys.—Solid State **1**, 136 (1959)]; G. L. Bir and G. E. Pikus, Fiz. Tverd. Tela **2**, 2287 (1960) [Sov. Phys.—Solid State **2**, 2039 (1960)].
[20]A. Cantarero, C. Trallero-Giner, and M. Cardona, Phys. Rev. B **39**, 8388 (1989).
[21]F. H. Pollak and M. Cardona, Phys. Rev. **172**, 816 (1968).
[22]R. C. Miller, D. A. Kleinman, and A. C. Gossard, Solid State Commun. **60**, 213 (1986); R. C. Miller, D. A. Kleinman, C. W. Tu, and S. K. Sputz, Phys. Rev. B **34**, 7444 (1986); D. A. Kleinman, R. C. Miller, and A. C. Gossard, *ibid.* **35**, 664 (1987).
[23]F. Agulló-Rueda, E. E. Méndez, and J. M. Hong, Phys. Rev. B **38**, 12 720 (1988).
[24]F. Cerdeira, E. Anastassakis, W. Kauschke, and M. Cardona, Phys. Rev. Lett. **57**, 3209 (1986).
[25]T. Ruf, C. Trallero-Giner, R. T. Phillips, and M. Cardona, Solid State Commun. **72**, 67 (1989).
[26]T. Ruf, R. T. Phillips, C. Trallero-Giner, and M. Cardona, following paper, Phys. Rev. B **41**, 3039 (1990).
[27]R. L. Aggarwal, Phys. Rev. B **2**, 446 (1970).
[28]R. Zeyher, C.-S. Ting, and J. L. Birman, Phys. Rev. B **10**, 1725 (1974).
[29]Y. Oka and M. Cardona, Solid State Commun. **30**, 447 (1979).
[30]C. Trallero-Giner, A. Alexandrou, and M. Cardona, Phys. Rev. B **38**, 10 744 (1988).
[31]*Physics of Group IV Elements and III-V Compounds,* Vol. 17a of *Landolt-Börnstein,* edited by O. Madelung, M. Schulz, and H. Weiss (Springer-Verlag, Berlin, 1982).
[32]M. Cardona, N. E. Christensen, and G. Fasol, Phys. Rev. B **38**, 1806 (1988).